Structure–property behaviour of segmented polyether–MDI–butanediol based urethanes: effect of composition ratio

S. Abouzahr and G. L. Wilkes
Department of Chemical Engineering, Virginia Polytechnic Institute and State University, Blacksburg, Virginia 24061, *USA*

and Z. Ophir
Celanese Research Company, Summit, New Jersey 07901, *USA*
(*Received* 14 *September* 1981)

The structure–property relationship of a systematic series of segmented polyurethanes was investigated segment was 4,4'-diphenylmethane diisocyanate (MDI) extended with 1,4-butanediol, and the soft segment was 2000 M_w poly(tetramethylene oxide) ether. X-ray studies reveal that some hard segment segment was 2000 mW poly(tetramethylene oxide) ether. X-ray studies reveal that some hard segment crystallization occurs at high hard segment content (45%). In addition, other morphological changes take place as the hard segment fraction is increased. The texture changes from that in which little such domain content exists at low hard segment levels (15%), to that in which the polymer has an interlocking domain morphology at high hard segment content (35 and 45%). Preferable elastomeric properties (low hysteresis, high extension) can be obtained when isolated hard segment domains exist (25% hard segment). Thermal treatment of the samples results in domain disruption and hard–soft segment mixing. However, this phenomenon, and the consequent time-dependent structure recovery as the material is allowed to age, is composition dependent. In general, crystalline domains, when present, are disrupted the least while the fastest recovery is displayed by samples with noncrystalline domain texture. This behaviour can be explained qualitatively in terms of kinetic diffusion effects relative to the thermodynamic driving forces for phase separation.

Keywords Polyurethane; segmented copolymers; thermoplastic elastomers; structure–property; elastomers; block copolymers

INTRODUCTION

Thermoplastic polyurethanes (TPU) are a broad class of macromolecules composed of chemically dissimilar units commonly denoted as hard and soft segments. Due to the extensive diversification of possible chemical constituents, a rather wide variety of mechanical properties can be obtained from these materials. The hard blocks in these systems generally associate at the use temperature to form small morphological distinct domains that serve as physical crosslinks and reinforcement sites[1–3]. Recent studies[4–6] have shown that this morphology is a function of several variables, examples being the composition ratio of the hard and soft segments, the molecular weight of the individual segments, component compatibility and symmetry, and the polymerization route (one or multi-step).

With regard to hard segment content for example, Critchfield, *et al.*[4] utilized dynamic mechanical testing to study the effect of hard segment content in 830 M_n and 2100 polycaprolactone diol with MDI and butanediol as the hard segments. Their data show that an increase in hard segment concentration, not unexpectedly, increases the modulus in the rubbery plateau region and shifts the T_g of the soft segment to higher temperatures. In addition, a considerable increase occurred in the breadth of the glass transition associated with the soft segment. The latter effect was less prominent for the higher molecular weight diol. Polymers based on the low molecular weight polycaprolactone diol exhibited progressively greater interactions with the hard segments at higher hard segment levels. It was suggested that increasing the hard segment content leads to more domain continuity, which accounts for the observed dynamic mechanical spectra. In a similar study from the same laboratory[7] the soft segment utilized was 2000 M_n poly(oxypropylene–oxyethylene) diol. It was found that variation in hard segment content from 60 to 65% (MDI + BDO), leads to a change in the material from that of a tough elastomeric polymer to a more brittle, high modulus plastic. This was attributed to possible segment mixing and phase inversion at high hard segment concentration. Regarding compositional effects on deformation behaviour, Cooper *et al.*[8] have used infra-red dichroism to study segmental orientation in polyurethanes with varied structures and composition. A significant change in orientation behaviour was seen in MDI–butanediol, with poly(tetramethylene ether) soft segment, when the MDI content was changed from 24 to 28%. The lower level of mechanical properties and orientability at 24% (MDI (33 wt% hard segment) was attributed to the inability of this material to form an interlocking domain structure. Similar conclusions have been made by Sung *et al.*[5] based on their i.r. dichroism data on poly(urethane ureas).

0032-3861/82/071077-10$03.00

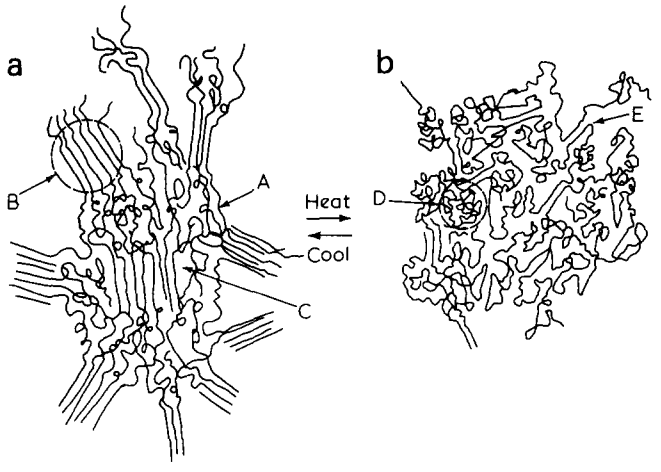

Figure 1 Schematic model depicting the morphology of segmented polyurethanes of both (a) well-aged, (b) annealed sample following heat treatment. A- partially extended soft segment; B- hard-segment domain; C- hard segment; D- coiled or 'relaxed' soft segment; E- lower-order hard segment domain

Over a range of composition variation, morphological changes in segmented elastomers induced by thermal treatment have been studied by Wilkes *et al.*[9-14], Cooper *et al.*[15-19], and Jacques[20] using the techniques of differential scanning calorimetry (d.s.c.), infra-red spectroscopy, tensile and dynamic mechanical analysis, small angle X-ray scattering (SAXS), wide angle X-ray scattering (WAXS), and nuclear magnetic resonance spectroscopy (n.m.r.). Wilkes *et al.*[9-14] have specifically investigated the kinetics of domain formation in several segmented polyurethanes. Samples which were heated briefly (5 min) near, or in, the processing range, and then quenched, exhibited concomitant changes in soft segment T_g, degree of phase separation (as evidenced by the SAXS), and Young's modulus as a function of post-quenching time. To explain this phenomenon, it was suggested that in giving many of the segmented urethanes a thermal pulse above 60°C, the domain texture is partially disrupted and segment mixing is promoted (*Figure 1*). At the annealing temperature, the domain morphology is less favoured thermodynamically than at a lower temperature. More specifically, the soft segments which had to be somewhat strained at lower temperature to allow phase separation, apply a retractive entropic stress at higher temperatures on the hard segments to which they are chemically bonded. This stress will increase as the temperature goes up (by classical rubber elasticity theory), along with the relative solubility of the two segments, resulting in domain disruption and segment mixing unless suitable hard segment symmetry exists as to promote crystallization. Upon quenching, a driving force for phase separation is again induced, but the demixing process is not instantaneous. At room temperature only the soft segments are above their T_g, while the hard segments are generally glassy and their mobility is necessarily low. The hard blocks are, therefore, rigid and their presence amidst the soft segments places restrictions upon the motion of the soft segment thereby increasing the soft segment T_g. One sees then that phase separation involves segmental transport processes through highly viscous and incompatible media and will therefore likely be composition dependent.

Jacques[20] has specifically studied the effect of high temperature annealing (150°–250°C) on the morphology of polyester polyurethane elastomers. D.s.c., i.r. spectroscopy, WAXS, and dynamic mechanical property analysis of crystallizable polyurethanes showed that annealing of control samples below 200°C resulted in long-range ordered hard segment domains at best (endotherm at 210°C) whereas annealing at 200°C and above lead to crystalline hard segment domains (melting at 249°C) with an associated dramatic increase in Young's modulus (up to 300%).

Seymour and Cooper[15-19] also studied the effect of annealing temperature (up to 200°C) and time on the thermal responses of polyester and polyether MDI–BD polyurethanes using d.s.c. analysis. In general, three hard segment associated endotherms were observed in untreated samples at temperatures of 60°–80°C, 120°–190°C and above 200°C. These endotherms were correlated respectively with short range, long range, and microcrystalline ordering of hard segment domains. Most recently, Cooper *et al.*[17] using calorimetric measurements further supported the earlier conclusions of those made by Wilkes and Jacques. The kinetics of phase separation was found to be dependent on the thermodynamic driving force for phase segregation and the viscosity of the material. If the polymer had highly ordered hard segment domains or was semicrystalline, domain disruption at high temperatures was significantly reduced, or even absent.

A related important mechanical property of these and other elastomeric systems is that of stress softening. In general, vulcanized or unvulcanized elastomers as well as their filled counterparts, require a greater stress to produce a given elongation in the first extension curve than during subsequent extensions[21]. This well-known phenomenon, particularly common to the segmented urethanes causes an appreciable amount of energy dissipation or mechanical hysteresis. In his attempt to account for this behaviour in segmented polyurethanes, Bonart used the SAXS method[22-24] to study hard segment orientation as a function of strain. Bonart proposed that the lamellar hard segment domains tend to orient at elongations below 200% with their long axis toward the stretch direction due to local torques acting through the 'force strands' of soft segments. Further stretching causes the hard segments to slip past one another, breaking up the original structure. As the elongation continues, the hard segments become progressively oriented in the stretch direction. More specrifically, Bonart suggests that this deformation and restructuring of the hard segments during elongation is related to stress softening and the observed hysteresis phenomena characteristic of these polymers. Sung *et al.*[5] have also demonstrated that hysteresis behaviour is a function of the extent of phase separation and composition in poly(urethane urea) elastomers. In filled elastomeric polymers, Dannenberg[25], Boonstra[26] and coworkers[27,28] suggested a slippage of the rubber network over the surface of the carbon black particles. Kraus *et al.*[29] considered the same effect to be the result of several mechanisms, including thixotropy involving transient carbon black structures, rupture of network chains connecting filler particles, and disruption of the 'permanent structure' of the carbon black. Harwood and Payne[30] have suggested that in unfilled rubber vulcanizates, stress softening does not necessarily involve

a breakdown process and is hence attributed to quasi-irreversible rearrangement of molecular networks due to localized non-affine deformation. This results from short chains reaching the limit of their extensibility leading to a relative displacement of the network junctions from their initial random state. In general, for leather-type materials[31] and for many other tougher elastomeric polyurethanes[26], the energy dissipation upon deformation has been associated with the movement of polymer chains, domain rearrangement and entanglement points when the sample is stressed. The permanent set obtained is due to the very wide distribution of relaxation times exhibited by the viscoelastic response of the polyurethane molecules and the presence of hydrogen bonds between neighbouring chains which become altered or broken under mechanical stress[26].

In general, and as will be discussed shortly, we believe stress-softening in segmented polyurethanes can likely be accounted for by three main mechanisms: (1) rearrangement of the rubbery network associated with slippate of entanglements and non-affine displacement of network points in the rubbery matrix; (2) structural changes of domain texture associated with the possible breakdown and reformation of hard segment domains; (3) breakage of weak 'crosslinks' such as hydrogen bonds.

This work focuses on the structure–property relationships of thermoplastic urethanes and the composition dependent morphology along with the final mechanical properties of these materials. It also considers the time- and temperature-dependent characteristics as well as the role of composition in governing the kinetics and the transformation of the texture upon ageing following a thermal treatment at 150°C.

EXPERIMENTAL

Mechanical properties

Mechanical property measurements included stress–strain, stress–relaxation, and tensile hysteresis and were performed using an Instron (Model 1122). Stress–relaxation experiments were carried out on well-aged or 'phase separated' samples as well as thermally annealed samples (domain texture has been disrupted) as follows. For the latter, aged samples were annealed for 10 min at 150°C and then quenched in ice water for one minute. Stress relaxation experiments were carried out after different intervals of ageing time at ambient temperature using a different sample in every test to ensure that no change in morphology was induced by previous tests. Tensile hysteresis experiments were made by stretching and unloading the dog-bone specimens to an increasing strain level for each cycle. The end of every cycle was concluded as the material displayed a zero stress. This way the polymer was not allowed to relax or further recover. Based on the initial sample length, the elongation rate was 50%/min and the strain levels were from 25 to 600%. The per cent hysteresis for a given cycle was calculated as the ratio of the area bounded by the loading–unloading curve to the total area under the corresponding stretching curve. The areas were calculated using a digital planimeter.

X-ray studies

Wide angle X-ray scattering (WAXS). A PW 1720 X-ray generator was utilized with a standard vacuum sealed Statton Camera.

Small angle X-ray scattering (SAXS). A standard Kratky small-angle X-ray camera was utilized for the SAXS experiments. The X-ray source was a Siemens AG Cu40/2 tube, operated at 40 kV and 25 MA. The generator was a General Electric XRD-6 unit, and cooling water at 65 ± 0.5°F was circulated by a Haskries cooler. Cu Kα monochromatic beam ($\lambda = 1.542$ Å) was obtained by Ni foil filtering. The counting of the X-ray intensity was performed by a Siemens sealed proportional gas detector, in conjunction with a pulse height analyser. The camera motor was controlled by a PDP/8a computer which also served for data acquisition. Two basic types of SAXS experiments were performed. The first type was the measurement at room temperature of the scattered intensity at a fixed angle as a function of post-annealing time. The fixed angle was chosen near the shoulder (or Bragg's maximum) of the SAXS curve. The time-dependent intensity served as a relative indicator of changes in the sample morphology. The data were normalized by:

$$I(t) = \frac{I(t) - I_b}{I_0 - I_b} \tag{1}$$

where $I(t)$ is the measured intensity, I_b is the background, and I_0 is the scattered intensity of the well-aged sample at the same scattering angle. This normalization eliminates the effects of different beam intensities, sample dimensions, and radiation absorption. The second type of SAXS experiment involved measuring the complete scattering curves. The data were utilized to calculate the mean swuate fluctuation in electron density, defined as[32]:

$$\langle \rho^2 \rangle = \frac{4\pi a^2 \tilde{Q}}{i_e N^2 t P_s} \tag{2}$$

where a is the sample to plane of registration distance (cm), i_e is the electron scattering cross-section $= 7.9 \times 10^{-26}$ cm^2, N is Avogadro's number, t is sample thickness (cm), P_s is the sample attenuated intensity of the primary beam and $\tilde{Q}$ is the invariant calculated using the smeared intensity and assuming the infinite slit approximation, i.e.,

$$\tilde{Q} = \int_0^\infty \theta \tilde{I}(\theta) \mathrm{d}\theta \tag{3}$$

where $\tilde{I}$ is the smeared scattered intensity and θ is the scattering angle. To calculate $\tilde{Q}$ from the raw data, a computer program written by C. Vonk was utilized[34].

Differential scanning calorimetry (d.s.c.)

Calorimetric studies were carried out on a Perkin-Elmer DSC-2 calorimeter. The heating range was 10°C per min and the full sensitivity was 5 mcal. The experiment involved measuring the soft segment glass transition temperature, T_g, which was taken as the inflection point of the transition.

Table 1 Properties and characteristics of the Et- samples

Sample	Hard segment fraction (wt %)	Soft segment *MW*	Soft segment T_g (°C)
1-Et-15-2	15	2000	−53
1-Et-25-2	25	2000	−56
1-Et-35-2	35	2000	−58
1-Et-45-2	45	2000	−61

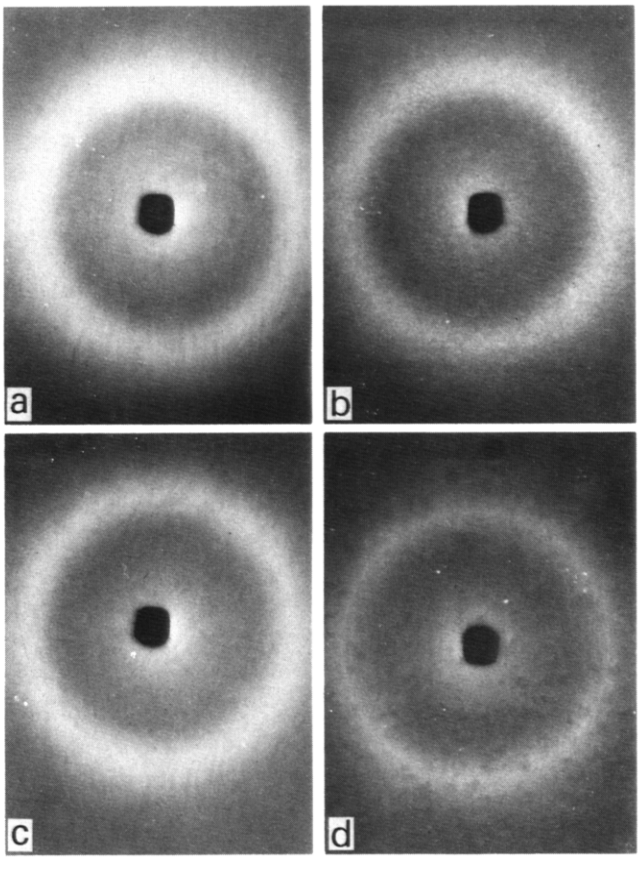

Figure 2 Wide angle X-ray diffraction patterns of the Et-series: (a) 1-Et-15-2; (b) 1-Et-25-2; (c) 1-Et-35-2; (d) 1-Et-45-2

Materials

A well-characterized and especially prepared series of polyether based urethanes was utilized for this study. The hard segment was *p,p'*-diphenylmethane diisocyanate (MDI) extended with 1,4-butanediol, and the soft segment was poly(tetramethylene oxide) glycol ($M_w \sim 2000$). The polymer was prepared via a one-stage polymerization process where the reactants were mixed and reacted randomly. The material then was compression moulded to produce films that were 0.06 cm thick. Four samples with different hard segment levels were prepared this way. These are listed in *Table 1*. The nomenclature used is as follows: e.g., 1-Et-15-2 represents a one-stage polymerization–polyether soft segment–15 wt% hard segment–2000 soft segment molecular weight. The polymer films were allowed to 'age' at room temperature for at least six months prior to any experimentation. Samples were then stored for one week *in vacuo* before the following study was carried out. All materials were kindly supplied and characterized following polymerization by Dr R. S. Schoellenberger of the B. F. Goodrich Center, Brecksville, Ohio.

The chemical structure of the hard segments, their concentration length and symmetry, are believed to be principally responsible for many of the viscoelastic properties displayed by segmented urethanes through the effects upon the domain texture and overall morphology of the material. The Et-series of segmented urethanes discussed below was specifically selected in order to study the morphological changes and associated mechanical properties as a function of increasing the hard segment content.

RESULTS AND DISCUSSION

X-ray diffraction and mechanical property studies

WAXS showed no distinct signs of crystallinity in any of the samples up to 35% hard segment content, as indicated by the absence of any sharp diffraction rings and the appearance of only a diffuse amorphous halo (*Figure 2*). Increasing the concentration of the hard segments, and consequently their length, enhances the structural arrangement of the hard segments and promotes some microcrystallinity of the domains as seen from the WAXS pattern of 1-Et-45-2 where some weak diffraction is observed. While WAXS results did not suggest any substantial crystallinity in samples having hard segment contents of 35% or less, the possibility of some small degree of crystallinity certainly cannot be ruled out. The consequences of this crystallizability will enter into our later discussion.

The absolute desmeared intensity SAXS scans of the Et series are shown in *Figure 3*. The area under the respective curve goes up as the hard segment content increases in this composition range, indirectly suggesting an increase in the volume fraction of hard domains. (More direct proof of this latter statement will follow.) *Figure 3* also reveals that only the curves of 1-Et-25-2 and 1-Et-45-2 show discrete or pronounced shoulders, while 1-Et-35-2 shows a broad but very weak shoulder and 1-Et-15-2 shows no

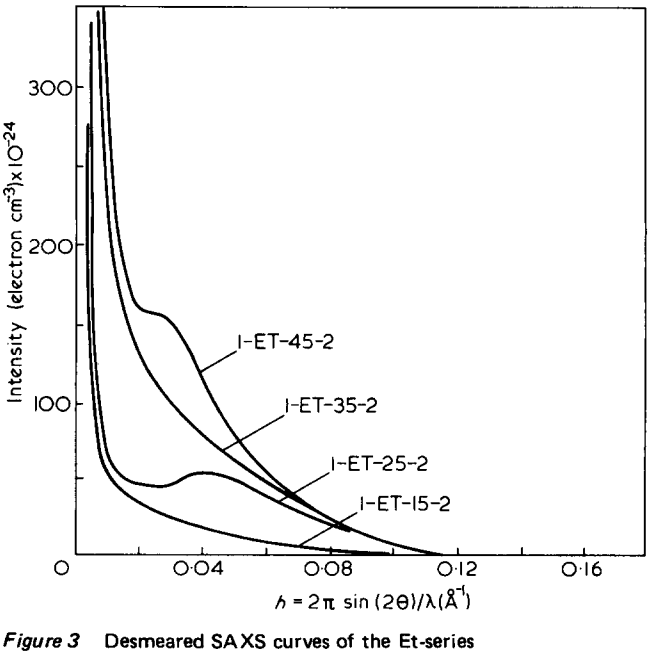

Figure 3 Desmeared SAXS curves of the Et-series

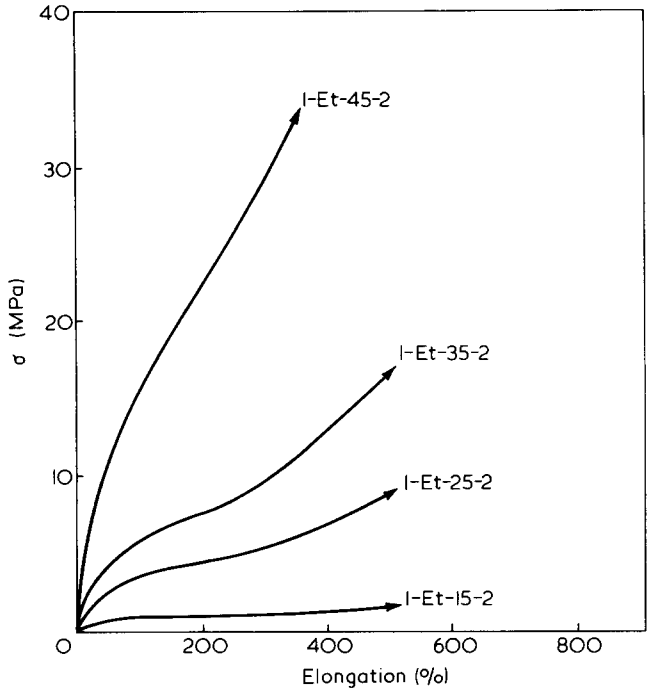

Figure 4 Stress–strain behaviour of the Et-series

observable peak or shoulder. These data suggest in turn that some degree of periodic structure exists in 1-Et-25-2 and 1-Et-45-2 and gives rise to the shoulder in the SAXS curves of these samples. However, the data suggest that no periodic order exists in 1-Et-15-2, while a broad distribution of domain sizes likely accounts for the absence of a distinct peak in the SAXS curves of 1-Et-35-2. It should also be pointed out that the change in the SAXS peak position of the samples is also consistent with the stoichiometry. That is, as the molecular weight of the soft segment is kept constant, increasing the hard segment amount results in an increase in the hard segment length. The result is an increase in the size of the hard domains and longer periodicities as evidenced by the shift of the side peaks to smaller angles in the SAXS scans. A similar observation in SAXS behaviour as affected by increased hard segment length has been noted in earlier work[9].

Additional information is gained when examining the stress–strain curves of the Et-samples in *Figure 4*. 1-Et-15-2 displays a rather low modulus that is characteristic of lightly crosslinked rubbers. 1-Et-25-2, however, shows good elastomeric properties that are reflected in a reasonably high modulus and good extensibility of the polymer. Both the 1-Et-35-2 and 1-Et-45-2 samples display behaviour that is characteristic of a tough plastic in that they have a high modulus but a rather low extensibility.

In *Figure 5*, both Young's modulus and the mean square in electron density fluctuation, $\langle\rho^2\rangle$, are plotted as a function of the hard segment concentration. It is observed that E increases as a nonlinear function of the hard segment weight fraction, w_1, indicating that the contribution of the hard segments is non-additive and hence some alteration in the morphology is taking place. *Figure 5* also reveals that both the behaviour of $\langle\rho^2\rangle$ and E approach a very low value at some positive quantity of w_1 (about 10%).

Inspecting *Figure 5* in some detail one notes that the functional behaviour of $\langle\rho^2\rangle$ with weight fraction is parabolic. This would be expected in the case of a well-phase-separated two-component system, for which the behaviour of $\langle\rho^2\rangle$ is described by the relationship:

$$\langle\rho^2\rangle = \varphi_1\varphi_2(\rho_1-\rho_2)^2 \tag{4}$$

where φ_1 and φ_2 are the respective volume fractions of components 1 and 2 which in turn have electron densities ρ_1 and ρ_2 (ref. 33). In our case we might let φ_1 and φ_2 be replaced by the weight fractions w_1 and w_2 if the densities are not very different. Doing this and realizing that $w_2 = 1 - w_1$ then rearranging equation (4) gives:

$$\langle\rho^2\rangle = -Aw_1^2 + Aw_1 \tag{5}$$

where A is $(\rho_1-\rho_2)^2$. This equation of course describes a parabola which displays a maximum at $w_1 = w_2 = 0.5$. Indeed while our own system is not completely phase separated nor do the weight fractions directly equal the volume fractions, the data of *Figure 5* clearly suggest that a maximum might be expected at about $w_1 = 0.5$. In view of this observation we also see that at a lower but finite w_1 ($\sim 10\%$), $\langle\rho^2\rangle$ would go to zero strongly implying that nearly 10% of the hard segments may be dissolved within the soft segment matrix rather than residing within discrete domains. Carrying this somewhat further, equation (5) can be rearranged to give:

$$\frac{\langle\rho^2\rangle}{w_1} = -Aw_1 + A \tag{6}$$

which suggests that plotting the left hand side against w_1 should provide a linear relationship and become zero when w_1 is equal to unity. Constructing this plot using

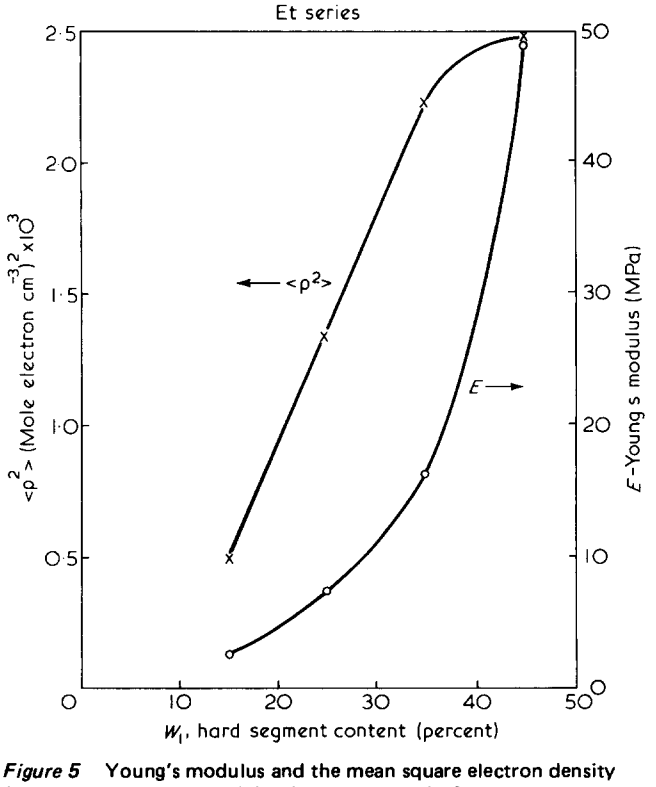

Figure 5 Young's modulus and the mean square electron density fluctuations variation with hard segment weight fraction

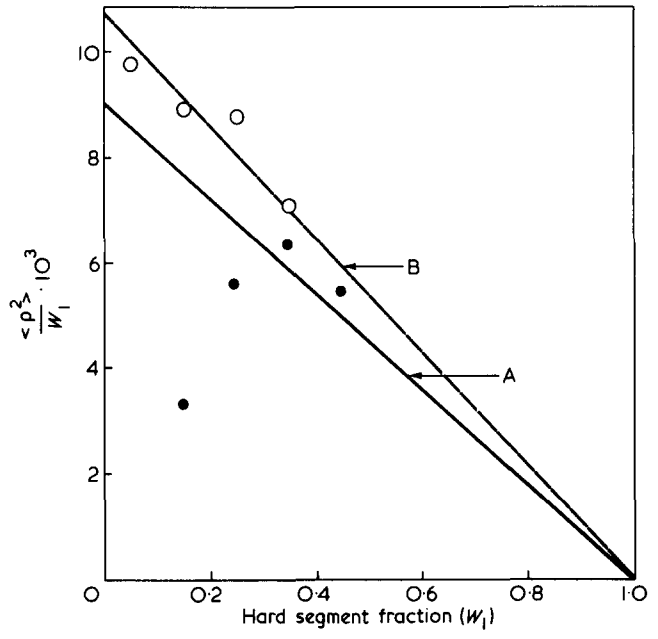

Figure 6 $\langle\rho^2\rangle/w_1$ as a function of w_1: A-actual data; B-w_1 was reduced by 10% for each sample

true values of w_1 provides *Figure 6* which basically provides some agreement with equation (4) in that the extrapolation to $w_1 = 1.0$ does suggest that $\langle\rho^2\rangle$ become zero. However, the deviation of the data at $w_1 = 0.15$ is very large thus making these data suspect. Interestingly if the values of w_1 are each reduced by 0.10 due to the observations made in *Figure 5* (i.e. at $\langle\rho^2\rangle$ equal to zero, w_1 is 0.10) then the second plot in *Figure 6* is obtained which provides much less scatter and is based on a better choice of values. In fact, it turns out that the observed deviation of any data point is now within experimental accuracy. In summary of the above treatment, although some of the assumptions utilized may be a bit bold, the trends clearly support a partial solubilization of the hard segments with the soft segments.

Based on the above information and the earlier discussion, a rather over-simplified morphological model for the Et-series is proposed and is shown schematically in *Figure 7*. It is speculated that in all the Et samples a small fraction of the hard segments are 'dissolved' in the soft phase possibly due to hard–soft blocks interaction (e.g. hydrogen bonding) and to the probably greater solubility of short hard segments in the rubbery matrix that result from the nature of the one-stage reaction process[34]. This means that for 1-Et-15-2, most of the hard segments are well mixed with soft segments and little periodic structure of the hard segment exists. Therefore, the modulus, as well as the scattered intensity is quite low. Upon stretching, the deformation is basically that of the soft rubbery material in that slippage of the polymer chains occurs due to little or no domain structure and the material exhibits a low modulus. As the hard segment fraction is increased to 25%, a sufficient amount of the hard segments 'nucleate' and phase separate to form isolated hard domains thus reinforcing and physically crosslinking the soft matrix so that the polymer displays good elastomeric properties characteristic of crosslinked rubbers. Clearly from the SAXS scan, some degree of periodic order exists in this system. A further increase of the hard segment concentration (1-Et-35-2) results in an increase in the lengths of the hard blocks and, consequently, in larger hard segment microphases. As these domains develop, some of them may touch each other to form longer and more irregular domains. The result is a broad distribution of domain sizes and shapes and is reflected in the lack of a pronounced 'Bragg' peak in the SAXS curve. In sample 1-Et-45-2, the amount of hard segments is high enough to form a new periodic structure (likely interconnected layers) that is reflected by the shoulder in the SAXS scan. The presence of crystallinity which plays an additional strengthening role at high hard segment content and the change from discrete domains to a continuous hard phase qualitatively explains the non-linear growth of E as the hard segment is increased. The interlocking domain texture in 1-Et-35-2 and 1-Et-45-2 contributes to the high modulus of these samples since the initial deformation involves a contribution of a continuous hard phase. The polymer, however, shows low extensibility since it behaves more like a rigid plastic.

Upon reinspecting the modulus data (*Figure 5*), they are somewhat reminiscent of those calculated from a simple series model composite where the modulus is given as:

$$E = E_1 E_2/(E_1\varphi_2 + E_2(1-\varphi_2)) \qquad (7)$$

where E is the modulus of the composite, φ_1 and φ_2 are the respective soft and hard segment volume fraction while E_1 and E_2 are the modulus of these same two components respectively. It is realized that the above relationship assumes a direct series addition of strains but equal stresses in the different phases and therefore represents the lower limit for a two-phase composite system. While our elements (domains and soft segment matrix) are not connected in series, this model provides a degree of similar behaviour as shown in *Figure 8* which was obtained by using equation (7) and 1000 MPa and 0.1 MPa for E_1 and E_1 respectively. These values were chosen since they are typical for crystalline and rubbery

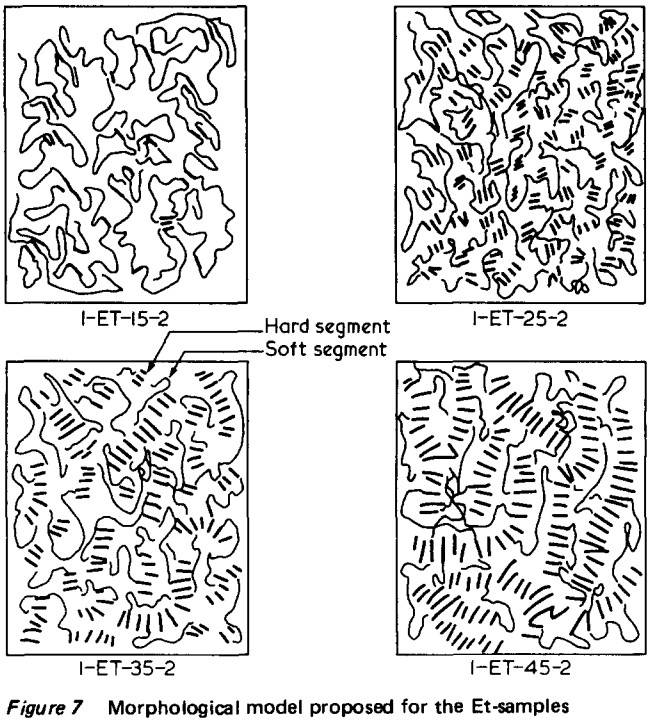

Figure 7 Morphological model proposed for the Et-samples

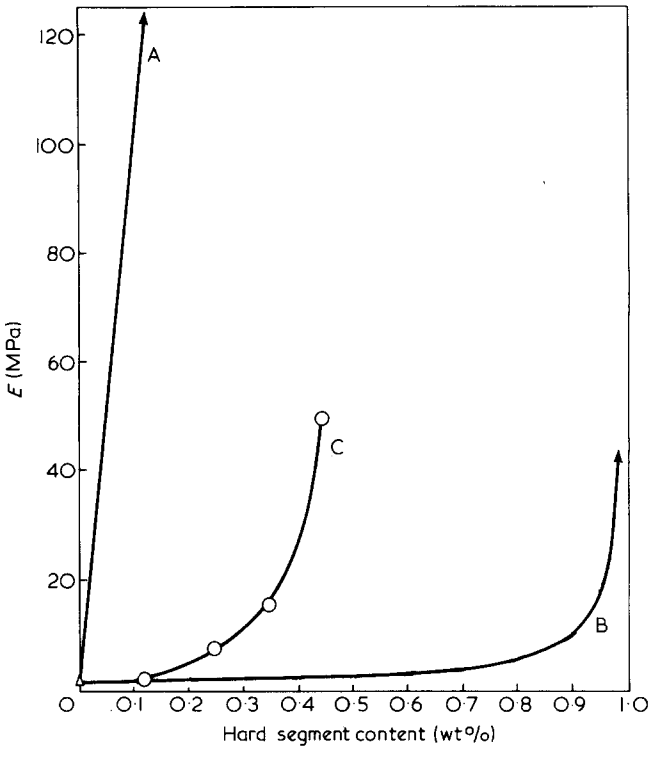

Figure 8 Young's modulus for (A) parallel model, (B) series model, (C) experimental data as a function of hard segment concentration

uncrosslinked polymers. Clearly the agreement is far from perfect in that the series model is somewhat lower in magnitude and deviates drastically from the experimental data. This difference is due to significant change in the morphological domain texture from that of distinct hard microphases to that of interpenetrating hard and soft segments.

In addition to the series model, the case where matrix and filler elements are considered to act in parallel is shown, i.e. the modulus of the composite is given by:

$$E=\varphi_1 E_1+\varphi_2 E_2 \qquad (8)$$

where all variables are as discussed before. Again, as expected, large deviation from the observed data (*Figure 8*) is noted since equation (8) assumes equal strain in both the matrix and the domains which is also highly unlikely. It is noted, however, that the experimental data fit an intermediate range of the above discussed models. Again, the explanation rests in terms of domain agglomeration and the morphological changes that occur as the hard segment content is increased and is expected in light of the SAXS analysis.

The above morphological models are consistent with the conclusions of Seymour and Cooper[15] who suggested on the basis of i.r. dichroism and mechanical experiments that a similar morphological transition occurs in a rather narrow composition range when the MDI content was changed from 24 to 28 weight per cent (about 33 wt% hard segment fraction). Specifically, they proposed[15] that when the hard segments are symmetric and their length is great enough to permit microcrystallinity, slightly negative segmental orientation results under uniaxial deformation conditions since the partly crystalline domains orient with their long dimension turning into the stretch direction while the hard segments that make up the domains are arranged perpendicular to the long dimension of the domain and accordingly take up a transverse orientation. Our own thoughts generally concur with these speculations although we do not feel that hard segment crystallinity must occur, i.e. non-crystalline domains of similar geometry might also display the same behaviour.

Mechanical hysteresis studies

Perhaps the most unique property of segmented polyurethanes is the microdomain two-phase morphology that is responsible for the phenomenon of thermo-plastic elastomeric behaviour. However, it has been suggested[23,24] that this same morphology is responsible for heat build-up in these polymers due to their high hysteresis losses. In general this property limits the utilization of these materials in certain applications where cyclic loading exists. We have attempted to shed some light on this phenomenon by studying the effect of increasing hard segment concentration on the hysteresis properties of this series of segmented polyurethanes. Hysteresis measurements were carried out under cyclic loading conditions as described earlier. *Figure 9a* shows that the lowest mechanical hysteresis is exhibited by 1-Et-25-2. 1-Et-35-2 and 1-Et-45-2 show very high hysteresis while 1-Et-15-2- shows hysteresis between that of 1-Et-25-2 and 1-Et-35-2. In addition, *Figure 9b* shows that the permanent set data follow the same pattern as the hysteresis data.

This behaviour for both mechanical properties can be reasonably explained qualitatively using the morphological models proposed earlier. Specifically, in 1-Et-15-2, the hard segments are relatively short and mostly solubilized in the soft segment matrix. Therefore, there are few physical crosslinks to prevent the polymer from flowing upon deformation. The result is high energy dissipation and permanent set. 1-Et-35-2 and 1-Et-45-2, however, contain hard segments with greater segment length. Due to more hard segment continuity, upon deformation the domains are disrupted causing a change in the network configuration. The mechanism of deformation involves high energy losses due to hard-segment orientation and an irreversible disruption of the molecular structure under stress, resulting in both higher hysteresis and permanent set. However, 1-Et-25-2 shows the best elastomeric properties and the lowest hysteresis due probably to its more isolated or discrete hard segment domains. Through this morphology, orientation effects are minimal and the deformation at low elongation is principally that of the soft segment. High hysteresis due to some partial domain distuption is likely at higher extension ratios.

Close examination of the hysteresis data reveals that the hysteresis curves of the different samples could be divided into more than one region depending upon the sample composition, which suggests that different mechanisms may be responsible for the hysteresis losses at different elongations. Specifically, the curve of 1-Et-25-2 could be divided into three reasonably distinct regions. The first, at low elongation $<50\%$ involves a rather high level of energy dissipation associated with non-affine deformation and orientation of hard segment domains. The second region (elongations between 50 and 500%) suggests some disruption of the domain texture and alignment of the hard segment backbones into the stretch

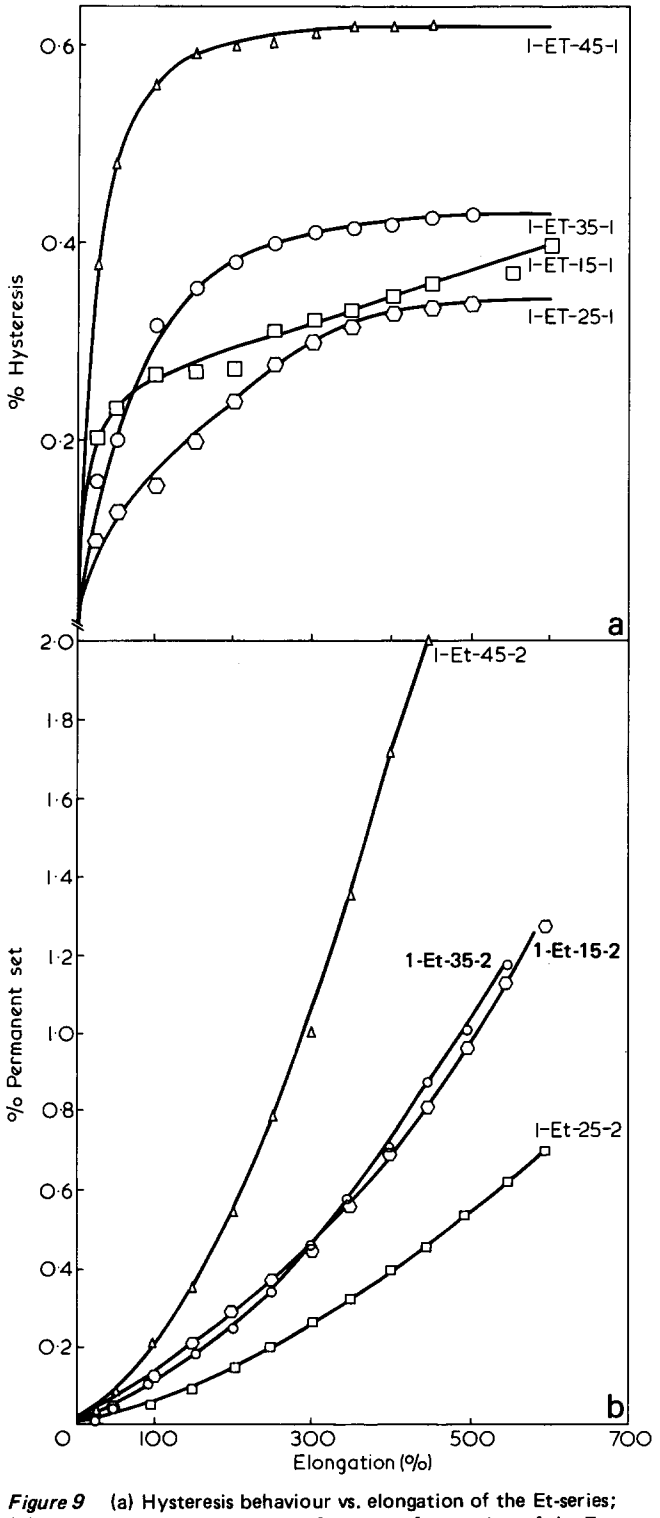

Figure 9 (a) Hysteresis behaviour vs. elongation of the Et-series; (b) permenant set behaviour as a function of extension of the Et-series

direction. The third region (> 500%) is that of a disrupted domain texture (in terms of hard phase continuity) and involves a constant level of hysteresis up to sample breakage and arises mainly from chain slippage and the different viscoelastic response of the hard and soft segments. However, since domain disruption occurs at low elongation at high hard segment concentration, both 1-Et-35-2 and 1-Et-45-2 display only two principal regions in their hysteresis behaviour. The first is that of domain disruption at low elongation (< 200% for 1-Et-45-2 and < 300% for 1-Et-35-2) and the second is that of mostly disrupted domain texture.

In summary, the hysteresis behaviour of urethane elastomers is found to be composition dependent. Several mechanisms account for the high energy losses in these systems. Which mechanism dominates is, however, a function of both hard segment concentration and extension ratio. Again we feel that our results are consistent with former studies cited but also provide additional structural information.

Time dependent studies

Time dependent properties were also followed by stress relaxation and SAXS measurements at ambient temperature (intensity at a fixed scattering angle) after giving the material a brief annealing treatment at 150°C for 10 min. The stress displayed by the material dropped to a lower value just after quenching and increased gradually to its original value as the material was allowed to age at room temperature (*Figure 10a–d*). This drop and recovery of the stress relaxation modulus is due to the mixing–demixing process of the hard and soft segments as outlined earlier. The stress reduction is due to the disruption of hard segment domains which arises from the thermal treatment. *Figures 11a* and *b* are the normalized SAXS intensities and normalized 100% modulus as a function of post-annealing time (the 100% modulus was normalized by its well-aged value) at the same elongation. Both plots show the same functional dependence and hence strongly indicate that these changes are related to the same physical process.

'Well aged' or control stress relaxation plots in particular tend to display two rather distinct stress relaxation regions. Initially the stress decays rapidly followed by a fairly slow relaxation rate (e.g. see *Figure 10b*). If one divides the overall curve into two components (percentage fast vs. slow component) the percentage of fast component goes through a minimum for the 1-Et-25-2 sample, indirectly suggesting a possible correlation to the hysteresis data where the same sample displayed the minimum loss. While we have not pursued this point further, we believe the correlation probably reflects the

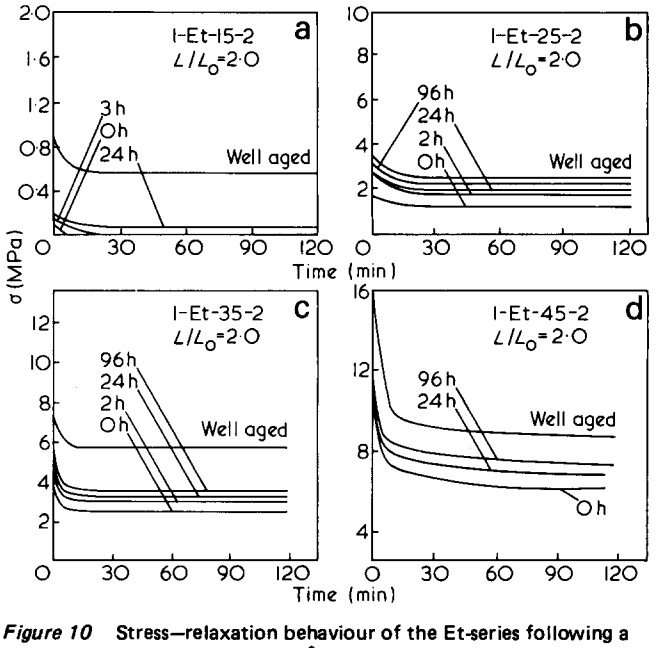

Figure 10 Stress–relaxation behaviour of the Et-series following a 10 min thermal treatment at 150°C

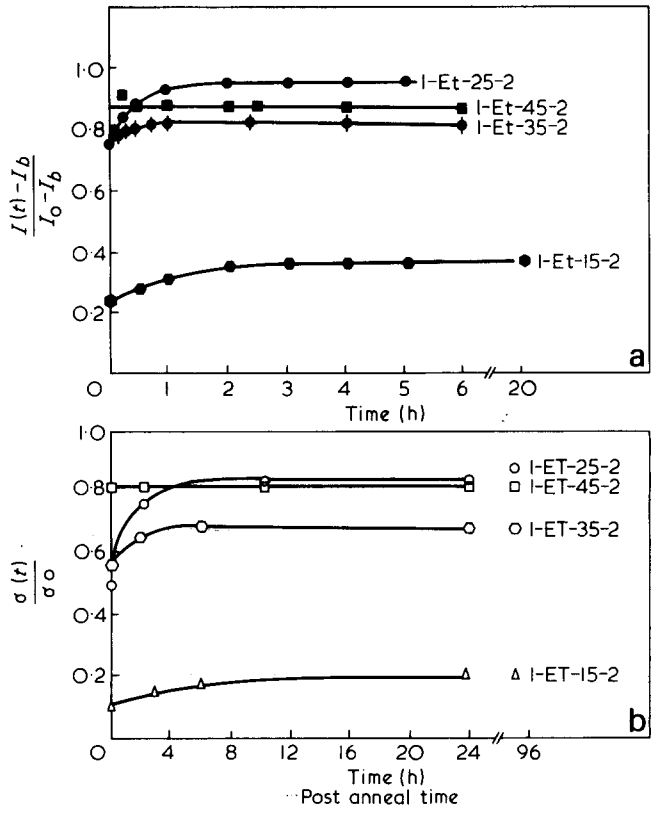

Figure 11 (a) Normalized fixed angle SAXS intensity of the Et-series following a 10 min thermal treatment at 150°C. (b) Normalized 100% Young's modulus of the Et-series following a 10 min thermal treatment at 150°C

same short time flow upon which the hysteresis behaviour also depends.

The earlier explanation regarding the morphology differences with composition is also applicable here in that the extent to which the morphology is disrupted, as well as the kinetics of microphase formation, is composition dependent. Both the normalized intensities and normalized stress at time zero (*Figures 11a* and *b*) show that the morphology of 1-Et-45-2 is disrupted least upon annealing since the stress and the scattered intensity values do not change significantly upon annealing, while that of 1-Et-15-2 is disrupted mostly due to its least perfect domain texture. Both 1-Et-35-2 and 1-Et-25-2 show an intermediate behaviour. As the hard segment content is increased, the morphology changes from that of discrete domains to that of a continuous hard segment. Annealing the polymer will then have a smaller effect on materials with high hard segment fractions than those of lower hard segment content, other factors being constant. Crystallization adds another consideration since hard segment crystallites (which definitely exist for 1-Et-45-2) would be less easily disrupted below the melting point. Furthermore, crystallization is a driving force for phase separation and hence high temperature annealing might favour phase separation by crystallization in contrast to segment mixing[17].

The demixing process is also influenced by composition. 1-Et-15-2 shows very slow recovery, since most of the hard blocks are solubilized in the soft matrix. The mutual solubility and interaction of the segments is rather high and restricts the movement of the short hard segments since the thermodynamics are less favourable. Increasing the hard segment fraction (and consequently the block length) increases the viscosity and hence reduces the mobility of the hard segments. This is shown in the behaviour of 1-Et-45-2, where the material shows little, if any, recovery after 96 h of post-annealing time. In 1-Et-25-2, however, both viscosity and solubility effects are relatively low and thermodynamics are quantitatively, at least, more favourable. The result is that upon ageing this sample displays the fastest recovery which is evident in the quick increase of the modulus and the scattered intensity.

D.s.c. studies

Complimentary d.s.c. studies were carried out to elucidate further the structure of the urethane samples under investigation. *Table 1* lists the glass transition temperature of the soft segment, T_g, of the different samples. Examination of *Table 1* reveals some striking results. The soft segment T_g surprisingly increases as the hard segment fraction decreases, i.e. 1-Et-15-2 shows the highest T_g.

This behaviour could be explained in light of the morphological models proposed earlier. Specifically, in the 1-Et-15-2 material, most of the hard segments are solubilized in the soft matrix and therefore will restrict the soft segments mobility and increase their T_g. As the hard segment length and concentration increase and discrete domains are formed, the surface area of the soft–hard segment contacts will actually decrease causing a decrease in the soft segment T_g. Similar results have been found by other workers[5] although this aspect of the data was not discussed in their paper.

CONCLUSION

The current work investigates the composition and time dependent morphology of segmented polyurethanes. Phase separation in these materials is very much a function of hard segment level. X-ray data support earlier studies where increasing hard segment fraction leads to microcrystallinity of the hard segment and results in phase inversion and domain continuity. Hysteresis behaviour reveals that different mechanisms account for stress softening in these segmented polyurethanes. Particularly, at high hard segment concentration, domain disruption dominates starting at low elongations. The material also displays high hysteresis possibly due to irreversible structuring of the morphology and high energy losses caused by hard-segment orientation. Samples thought to possess rather distinct domain texture show the lowest hysteresis characteristics while those with no domain texture show an increasing level of hysteresis with strain. This is explained in terms of a morphological model in which the domains act as effective crosslinks and filler particles that physically crosslink and reinforce the soft segment matrix. Giving the material a thermal treatment at 150°C causes domain disruption and promotes segment mixing. The kinetics of domain formation was found to be dependent on the driving force for segment segregation and the viscoelastic properties of the material. At hard high segment content where the polymer possesses semi-crystalline domains, the disruption of the morphology at high temperatures was significantly reduced and the phase separation process was hindered, possibly due to the higher viscosity of the

material and the structural stability of the semi-crystalline regions.

ACKNOWLEDGEMENT

The authors wish to acknowledge the financial support of the National Science Foundation – Polymer Materials Division – for this study.

REFERENCES

1 Cooper, S. L. and Tobolsky, A. V. *J. Appl. Polym. Sci.* 1966, **10**, 1837
2 Estes, G. M., Cooper, S. L. and Tobolsky, A. V. *J. Macromol. Sci.* 1970, **4(2)**, 313
3 Van Bogart, J. W. C., Lilaonitkul, A. and Cooper, S. L. *Adv. Chem. Ser.* 1978, **176**, 1
4 Seefried, C. G., Koleske, J. V. and Critchfield, F. E. *J. Appl. Polym. Sci.* 1975, **19**, 2503
5 Sung, C. S. P. 'Polym. Alloys II' (Eds. D. Klempner and K. C. Frisch), Plenum Publishing Co., 1980
6 Abouzahr, S. and Wilkes, G. L. in preparation
7 Zolrahala, R. J., Gerkin, R. M., Hager, S. L. and Critchfield, I. E. *J. Appl. Polym. Sci.* 1979, **24**, 2041
8 Hun, D. S. and Cooper, S. L. *Polym. Eng. Sci.* 1971, **11(5)**, 369
9 Samuel, S. L. and Wilkes, G. L. *J. Polym. Sci.* 1973, **A2, 11**, 807
10 Wildnauer, R. and Wilkes, G. L. *Polym. Prepr. Am. Chem. Soc. Div. Polym. Chem.* 1975, **16**, 600
11 Wilkes, G. L., Bagrodia, S., Humphries, W. and Wildnauer, R. *J. Polym. Lett.* 1975, **13**, 321
12 Wilkes, G. L. and Wildnauer, R. *J. Appl. Phys.* 1975, **46**, 4148
13 Assink, R. A. and Wilkes, G. L. *Polym. Eng. Sci.* 1977, **17**, 606
14 Ophir, Z. H. and Wilkes, G. L. *Adv. Chem. Ser. Am. Chem. Soc.* 1978, **176**, 53
15 Seymour, R. W. and Cooper, S. L. *Macromolecules* 1973, **6**, 48
16 Ng, H. N., Allegrezza, A. E., Seymour, R. W. and Cooper, S. L. *Polymer* 1973, **14**, 255
17 Hesketh, T. R., Van Bogart, J. W. C. and Cooper, S. L. *Polym. Eng. Sci.* 1980, **20(3)**, 190
18 Lilaonitkul, A., West, J. C. and Cooper, S. L. *J. Macromol. Sci. Phys.* 1976, **B12**, 563
19 Hesketh, T. R. and Cooper, S. L. *Org. Coatings Plast. Chem., Am. Chem. Soc.* 1977, **37**, 509
20 Jacques, C. H. M. 'Polymer Alloys, Blends, Blocks, Grafts, and Interpenetrating Networks' (Eds. Daniel Klempner and Kurt C. Frisch), Plenum Press, NY, 1977
21 Payne, A. R. *J. Polym. Sci. Symp.* 1974, **48**, 169
22 Bonart, R. *J. Macromol. Sci. Phys.* 1968, **B2(1)**, 115
23 Bonart, R., Morbitzer, L. and Hentze, G. *J. Macromol. Sci. Phys.* 1969, **B3(2)**, 337
24 Bonart, R., Morbitzer, L. and Muller, E. H. *J. Macromol. Sci. Phys.* 1974, **B9(3)**, 447
25 Dannenberg, E. M. *Trans. IRI* 1966, **42**, T26
26 Boonstra, B. B. 'Reinforcement of Elastomers' (Ed. G. Kraus), Interscience, 1965
27 Dannenberg, E. M. and Brennan, J. J. *Rubber Chem. Technol.* 1966, **39**, 597
28 Brennan, J. J., Jermyn, T. E. and Perdagio, M. F. *ACS Div. Rubber Chem.* 1964, Paper No. 36, Detroit
29 Kraus, G., Childers, C. W. and Rollman, K. W. *J. Appl. Polym. Sci.* 1966, **10**, 229
30 Harwood, J. A. C. and Payne, A. R. *J. Appl. Polym. Sci.* 1966, **10**, 315
31 Payne, A. R. and Popplewell, D. *SATRA Poromerics Symp.* 1968, Corby, SATRA Publication, p. 204
32 Brown, D. S. and Wetton, R. E. 'Polymer Characterization' (Ed. J. V. Dawkins), Applied Science Publishers Ltd, Essex, England, 1980
33 Alexander, L. E. 'X-Ray Diffraction Methods in Polymer Science', Wiley–Interscience, John Wiley and Sons, Inc., 1969
34 Peebles, L. H. *Macromolecules* 1976, **9**, 58